

Feedback Control with Central Pattern Generator for Decentralized Coordination of Prototype Mechanical Rectifier

T. Iwasaki and B. Liu

Department of Mechanical and Aerospace Engineering
University of Virginia, 122 Engineer's Way
Charlottesville, VA 22904-4746
Email: iwasaki@virginia.edu

Abstract—This paper proposes a prototype mechanical rectifier (PMR) that captures essential dynamics underlying animal locomotion by a simple pendulum-disk configuration. We use the PMR to study the control mechanism of animal locomotion. In particular, we shall verify via numerical experiments the prediction from biological observations that a central pattern generator (CPG) with a decentralized structure is capable of coordinating the body motion to achieve locomotion with the aid of sensory feedback. The efficiency of locomotion achieved by the decentralized CPG is also investigated in comparison with analytical results we derive for statically optimal locomotion.

I. INTRODUCTION

Most animal locomotions such as walking, swimming, crawling, and flying, are achieved by periodic motion of the body, coupled with the surrounding environment to generate propelling force. For instance, a snake crawls by undulating its body on the ground, while a bird flies by flapping its wings in the air. The coupled body-environment system may be conceived as a “mechanical rectifier” that converts a periodic motion input to a biased forward velocity [1]. Biologists have found evidence that rhythmic animal motions are generated through muscle contractions commanded by certain neuronal elements called central pattern generators (CPGs). Thus, animal locomotion is realized by effective coupling of a CPG and a mechanical rectifier.

The CPG is a biological oscillator consisting of a group of neurons networked in a specific way that allows for generation of stable limit cycles with appropriate phase and frequency. In effect, the CPG is a neuronal controller that drives the mechanical rectifier to achieve certain animal locomotion. The architecture of CPGs (i.e., how the neurons are connected) has been extensively studied for a wide variety of animals, and their mathematical models have been developed and validated through carefully designed experiments [2]–[4]. Thus, significant knowledge has been generated through experimental studies to explain how biological motion control systems work.

Until very recently, the flow of information through the nerve cord has been believed to be essential to coordinate oscillations of various body parts to generate locomotion (see

e.g. [5] for a survey). However, recent study [6] by Yu *et al.* showed that it is not true. They examined experimentally how the swimming motion of leeches is affected when the nerve cord is severed at the mid-cord. Surprisingly, the coordinated undulatory locomotion continued to be observed afterward, albeit with greater than normal phase lags. This means that the information necessary for coordination can flow through the body as mechanical signals, and each of anterior and posterior CPGs is capable of extracting the information to determine an appropriate phase. Thus, CPGs can achieve coordination without directly communicating to each other with the aid of sensory feedback. From an engineering view point, *this suggests possibility for decentralized feedback control of mechanical locomotion systems.*

The main objective of this paper is to validate the prediction that a CPG-based feedback controller with a decentralized structure is capable of coordinating the motion of a mechanical rectifier to achieve locomotion. To this end, we shall first develop a prototype mechanical rectifier (PMR) that captures essential dynamics of the coupled body-environment system for animal locomotion. The PMR consists of a double pendulum and a rotating disk, and this simple structure allows us to see how the rectification occurs through the interaction between the body (pendulum) and the environment (disk). We will then develop a CPG-based controller with a decentralized structure using the reciprocal inhibition oscillator (RIO) [7]–[9] as a basic unit. Most parameters of the controller and the PMR are fixed to some nominal values through nondimensionalization. A few parameters remained are used to study the behavior of the closed-loop CPG-PMR system.

Our first result confirms that locomotion of the PMR can be achieved by the decentralized CPG for a range of parameter values. If biological systems have evolved to optimize a certain property such as energy efficiency, we would expect to find some optimality in our CPG-based controller. If so, the question is: what would be the cost function optimized by the CPG-based controller? We attempt to answer this question by developing an analytical characterization of statically optimal locomotion and comparing observations from numerical experiments with the optimal behavior.

II. PROTOTYPE MECHANICAL RECTIFIER

A. Overview

Consider a mechanical system composed of a double pendulum and a rotating disk as shown in Fig. 1. The pivot O of the pendulum is fixed to the inertial frame, and the two joints O and A are equipped with DC motors to generate torques u_1 and u_2 and optical encoders to measure the angular displacements θ_1 and θ_2 . The tip of the pendulum B is not fixed to, but just touches, the disk, and exerts friction force on the disk. The center of the disk is fixed to the inertial frame through a bearing and the disk can rotate around C .

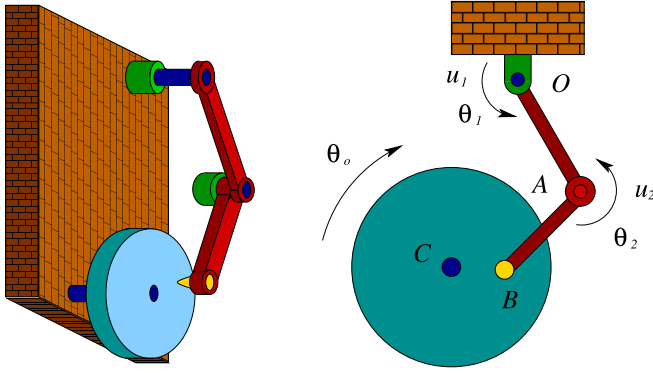


Fig. 1. Prototype mechanical rectifier (PMR)

The intended operation of the system is basically to swing the pendulum to make the disk rotate. The closest analogy would probably be human legs trying to propel a bicycle. Since the tip B of the pendulum is not fixed to the disk, there are three degrees of freedom instead of one, and the dynamics is more complex than riding on a bike. In fact, the system captures the essential dynamics of many forms of animal locomotion. The key is that oscillatory motion of the body (the pendulum) can generate locomotion (steady rotation of the disk) if and only if the oscillations of body parts are appropriately coordinated. This property motivates us to call the system a PMR.

B. Basic model

The differential equations governing the motion of the PMR can be derived through an application of the first principle. For simplicity, we impose the following:

Assumption 1:

- Each link has a uniform mass distribution and the both links have the same mass density and an identical shape (i.e., proportional dimensions).
- There are frictions at the disk bearing C and the contact point B between the disk and the pendulum, and their magnitudes are proportional to the angular velocity of the disk and the relative velocity between the pendulum tip and point B on the disk, respectively.

Under these assumptions, the equations of motion, after a normalization, can be given by

$$\begin{aligned} J_\theta \ddot{\theta} + G_\theta \dot{\theta}^2 + c V_\theta^\top (V_\theta \dot{\theta} + v_\theta \dot{\theta}_o) + h_\theta g &= Bu, \\ J_o \ddot{\theta}_o + c v_\theta^\top (V_\theta \dot{\theta} + v_\theta \dot{\theta}_o) + \dot{\theta}_o &= 0, \end{aligned} \quad (1)$$

where the time axis is scaled as $\tau := c_b t$ and

$$\begin{aligned} \theta &:= \begin{bmatrix} \theta_1 \\ \theta_2 \end{bmatrix}, \quad u := \begin{bmatrix} u_1 \\ u_2 \end{bmatrix}, \quad \Omega_\theta := \begin{bmatrix} \cos \theta_1 & \cos \theta_2 \\ \sin \theta_1 & \sin \theta_2 \end{bmatrix}, \\ C_\theta &:= \begin{bmatrix} \cos \theta_1 & 0 \\ 0 & \cos \theta_2 \end{bmatrix}, \quad S_\theta := \begin{bmatrix} \sin \theta_1 & 0 \\ 0 & \sin \theta_2 \end{bmatrix}, \\ B &:= \begin{bmatrix} 1 & -1 \\ 0 & 1 \end{bmatrix}, \quad e := \begin{bmatrix} 1 \\ 1 \end{bmatrix}, \quad z_c := \begin{bmatrix} y_c/\ell_1 \\ -x_c/\ell_1 \end{bmatrix}, \\ c_c &:= c_c(\ell_1^2/J_1), \quad c_b := c_b/J_1, \quad c := c_c/c_b, \quad \alpha := \ell_2/\ell_1, \\ J_o &:= J_o/J_1, \quad g := g/(\ell_1 c_b^2), \quad u(\tau) := u(t)/(J_1 c_b^2), \\ J_\theta &:= J + S_\theta H S_\theta + C_\theta H C_\theta, \quad G_\theta := S_\theta H C_\theta - C_\theta H S_\theta, \\ V_\theta &:= \Omega_\theta L, \quad v_\theta := \Omega_\theta L e + z_c, \quad h_\theta := S_\theta h, \\ J &:= \begin{bmatrix} 1 & 0 \\ 0 & \alpha^5 \end{bmatrix}, \quad H := 3 \begin{bmatrix} 1 + 4\alpha^3 & 2\alpha^4 \\ 2\alpha^4 & \alpha^5 \end{bmatrix}, \\ h &:= 6 \begin{bmatrix} 1 + 2\alpha^3 \\ \alpha^4 \end{bmatrix}, \quad L := \begin{bmatrix} 1 & 0 \\ 0 & \alpha \end{bmatrix}, \end{aligned}$$

and the variables and parameters are summarized below.

θ_o	rotational angle of disk
θ_1, θ_2	link angles from downward vertical
u_1, u_2	torque inputs
ℓ_1, ℓ_2	link lengths
(x_c, y_c)	coordinate of disk center (O is the origin)
c_b, c_c	friction coefficients at bearing and contact
J_o, J_1, J_2	moments of inertia for disk and links

Clearly, the first equation in (1) is for the pendulum, while the second for the disk. The torque input u generates periodic motion θ of the double pendulum which in turn interacts with the disk through a frictional coupling to yield its rotation with velocity $\dot{\theta}_o$. Thus the PMR represents typical dynamics found in animal locomotion where periodic body motion, interacting with the environment, produces biased velocity. Indeed, mathematical models of an n -link robotic snake [10], [11] also have this exact structure.

C. Statically optimal locomotion of PMR

In this section, we shall discuss optimal locomotion of the PMR. Reasonable ways to define the notion of optimality are not unique. For instance, it may be defined by minimality of the average power $\dot{\theta}^\top B u$ over a cycle supplied as the torque input u to achieve a given locomotion speed $\dot{\theta}_o$. Alternatively, the average value of $\|u\|^2 - \dot{\theta}_o^2$ in the steady state may be used as the cost function to be minimized. Our interest here is to define a particular cost function in such a way that the locomotion achieved by our CPG-based

controller is close to the optimum with respect to the chosen criterion. In other words, we look for a criterion with which a CPG-based controller seems to optimize the locomotion.

Among the criteria we have considered, including the kinetic energy and the energy loss due to the frictions, the average value of the pendulum tip speed $\|v_{\text{tip}}\|$ during locomotion at a given speed $\dot{\theta}_o = \omega_o$ turns out to be the best candidate for the cost function minimized by CPG-based controllers.

Let us formalize the optimality criterion as follows.

Definition 1: A function $\theta(t)$ is called a *trajectory* of the PMR if it satisfies (1) for some $u(t)$ and $\theta_o(t)$. A trajectory $\theta(t)$ of the PMR is called a *statically optimal trajectory* with locomotion speed ω_o if it possesses the following properties:

- (a) $\dot{\theta}_o(t) \equiv \omega_o$ for all t .
- (b) At every time instant, $\dot{\theta}(t)$ minimizes $\|v_{\text{tip}}(t)\|$.
- (c) The initial condition $\theta(0)$ minimizes the average value of $\|v_{\text{tip}}(t)\|$ in the steady state.

Property (a) means that the PMR locomotion is achieved at a constant disk speed of ω_o . Property (b) specifies $\dot{\theta}$ as a function of θ at every time instant, and thus the trajectory is completely determined once an initial condition is given. Property (c) states how the initial condition should be chosen.

It would be more natural to consider a dynamically (rather than statically) optimal trajectory that minimizes the average value of $\|v_{\text{tip}}\|$ during the steady state locomotion with speed ω_o . However, it seems difficult to obtain a simple characterization of the dynamically optimal trajectory. On the other hand, if we consider a statically optimal trajectory as above, we can obtain clean analytical results that are useful for examining optimality of CPG-induced locomotion as shown below.

Let us first consider the class of trajectories that have Properties (a) and (b). It can be verified that the cost function is expressed as $\|v_{\text{tip}}\| = \|V_\theta \dot{\theta}\|$. So the problem is to minimize this expression subject to (1) and $\dot{\theta}_o(t) \equiv \omega_o$. Noting that B in (1) is invertible and u does not appear explicitly in the cost function $\|V_\theta \dot{\theta}\|$, we may ignore the first equation in (1) and concentrate on the trajectory optimization based on the second equation. This is because any smooth trajectory can be generated by an appropriate choice of u due to invertibility of B . So we formulate the following problem:

$$\min_{\dot{\theta}} \|V_\theta \dot{\theta}\| \quad \text{subject to} \quad c v_\theta^\top (V_\theta \dot{\theta} + v_\theta \omega_o) + \omega_o = 0 \quad (2)$$

where $\omega_o \neq 0$ is a given (constant) locomotion velocity. This is a static optimization problem in which we choose the best $\dot{\theta}(t)$ based on the current state $\theta(t)$. It turns out that the optimal dynamics $\dot{\theta} = f(\theta)$ chosen in this way gives rise to a periodic solution with constant $\|v_{\text{tip}}(t)\|$. The initial condition $\theta(0)$ can then be chosen to minimize $\|v_{\text{tip}}(t)\|$ to satisfy Property (c). Thus we have the following result.

Theorem 1: *Let $\omega_o \neq 0$ and a trajectory $\theta(t)$ of the PMR be given. Suppose that the double pendulum does not become*

straight along the trajectory. Then it is a statically optimal trajectory with locomotion speed ω_o if and only if

$$\dot{\theta} = -2\omega_o V_\theta^{-1} v_\theta, \quad \|v_\theta(0)\| = 1/\sqrt{c}.$$

In this case, we have

$$v_\theta(t) = \begin{bmatrix} \cos \omega t & \sin \omega t \\ -\sin \omega t & \cos \omega t \end{bmatrix} v_\theta(0), \quad \omega := 2\omega_o.$$

Thus the tip of the double pendulum rotates in a circular orbit with radius $1/\sqrt{c}$ and frequency $2\omega_o$. Moreover, the tip speed $\|v_{\text{tip}}\|$ is constant and is given by

$$\|V_\theta \dot{\theta}\| = 2\omega_o/\sqrt{c}.$$

We remark that, if the objective function in (2) is replaced by the instantaneous power loss due to the friction, $c\|V_\theta \dot{\theta} + v_\theta \omega_o\| + \omega_o^2$, then the corresponding statically optimal trajectory is exactly the same as the one in Theorem 1 except for the initial condition $\|v_\theta(0)\|$. The best choice for $\|v_\theta(0)\|$ to minimize the power loss is the physically allowable maximum value, $1 + \alpha - \|z_c\|^2$, which occurs when the pendulum is straight and passes through the disk center. In this case, however, the trajectory is no longer well defined due to the singularity of V_θ .

III. CPG-BASED FEEDBACK CONTROL

The objective of this section is to develop an architecture for CPG-based controllers with a decentralized structure, based on the knowledge from the biological literature.

A. Neuron model

The neuronal dynamics can be modeled as an input-output system $v = \mathcal{N}(i)$ from the current injection input i to the membrane potential output v [12]. A structure for the neuron model may be given by

$$v = \mathcal{A}(q), \quad q = \mathcal{F}(i)$$

where \mathcal{A} and \mathcal{F} represent the dynamical mappings of the axon and the soma/dendrites part, respectively, and q is the current flowing from the soma to the axon.

In this paper, we adopt the Lur'e model for neuronal dynamics [13], [14], in which \mathcal{F} is given by

$$F(s) = \frac{ks}{(1 + \tau_1 s)(1 + \tau_2 s)}$$

and \mathcal{A} is given by

$$\begin{aligned} \tau_v \dot{v} &= \psi_1(v) - w + q \\ \tau_w \dot{w} &= \psi_2(v) - w \end{aligned} \quad (3)$$

where functions ψ_k ($k = 1, 2$) are defined by

$$\begin{aligned} \psi_1(v) &= c\phi(av) + q_o - bv \\ \psi_2(v) &= \phi(d(v + v_o)) \end{aligned}, \quad \phi(x) := \frac{1}{1 + e^{2-4x}}.$$

Note that ϕ is a sigmoid function (i.e., monotonically increasing and bounded). All the parameters except for q_o and v_o are positive, leading to “N-shaped” $-\psi_1$ and sigmoidal ψ_2 .

B. Reciprocal inhibition oscillator

The reciprocal inhibition oscillator is the simplest CPG consisting of two neurons with mutually inhibitory synaptic connections [8]. The block diagram of the RIO is shown in Fig. 2 where two neurons \mathcal{N} are connected via inhibitory synapses with strength σ . Note that the RIO has inputs r_i and outputs v_i ($i = 1, 2$).

Fig. 3 shows the time response of an RIO when an impulse input is applied to r_2 . As shown, the typical response is given by alternating oscillations in v_1 and v_2 with 180 degree phase difference. In this simulation, the impulse is of intensity 1, and the model parameters are taken from [15], [16] with a modification that the time axis and the membrane potential variable v are scaled so that the period of the RIO oscillation is 2π and the integral of v_1 over one period is 2 (which is the area under the sinusoidal curve $\sin t$ ($0 \leq t \leq \pi$)). The parameter values are summarized in Appendix.

This RIO is bistable when the inputs are zero, with a stable equilibrium and a stable limit cycle (spike train). The impulse input pushes the states from the equilibrium into the domain of attraction of the limit cycle. The condition on the RIO parameters for existence of an oscillatory solution has been obtained in [16].

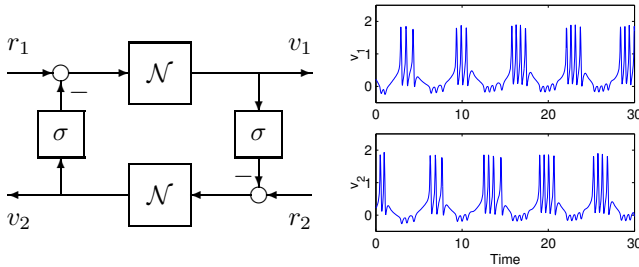


Fig. 2. RIO

Fig. 3. Oscillation profile of the RIO

C. Decentralized control architecture

The RIO described in the previous section is used to drive the PMR. All the RIO parameters are fixed as in Appendix except for the base frequency ϖ which remains as a design parameter. Recall that the PMR can be actuated through the two torque inputs u_i ($i = 1, 2$) at the pivot and joint of the double pendulum. We assume that the relative angles

$$\phi_1 := \theta_1, \quad \phi_2 := \theta_2 - \theta_1$$

are measured and conditioned through nonlinearities

$$\varphi_i(\phi) := a_i \tanh(b_i(\phi - \phi_{i0}))$$

where a_i and b_i are positive constants and ϕ_{i0} are the nominal relative angles. We shall drive each input u_i by an RIO based on the sensory signal through the feedback gain κ_i as shown in Fig. 4. Note that this is essentially a positive feedback where the positive/negative $\phi_i - \phi_{i0}$ tends to generate positive/negative u_i .

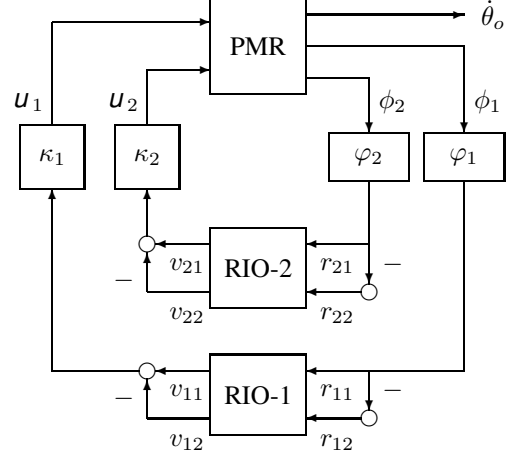


Fig. 4. CPG-based control system

The CPG consists of the two RIOs and has a decentralized structure, i.e., there is no direct communication path between the RIOs. Based on the biological observation of leech swimming, we expect that the decentralized CPG is capable of inducing locomotion of PMR. In particular, the information from the sensory feedback should be enough to coordinate the RIO oscillations.

IV. NUMERICAL EXPERIMENTS

This section examines feasibility/optimality properties of the CPG-based control architecture developed in the previous section through numerical experiments. In particular, we assess whether there exists a set of controller parameters that yields locomotion of the PMR, and, if so, study optimality properties of CPG-induced PMR locomotion.

We conduct numerical experiments of the control system in Fig. 4. We use an identical system for both RIO-1 and RIO-2, which is given by the block diagram in Fig. 2 where the neuron model \mathcal{N} is as described in Section III-A with parameters in Appendix. In this preliminary study, we consider the simple case where $\kappa_1 = \kappa_2 =: \kappa$. The normalized PMR model (1) is used in the simulation. We assume that there is no gravity $\mathbf{g} = 0$. In this case, we can assume $x_c = 0$ without loss of generality by choosing an appropriate coordinate system. The remaining PMR parameters are chosen to yield a generic configuration; the two links of the double pendulum have the same length ($\alpha = 1$), the disk center is located at the three-quarter of the total pendulum length from the pivot ($y_c = -1.5$), the moment of inertia for the disk is several times larger than the link ($J_o = 5$).

Throughout the experiments, the impulse input $p\delta(t)$ is applied to the RIOs through r_{12} and r_{21} channels to initiate the RIO oscillation when the system is at rest in the nominal configuration. The intensity p is chosen slightly above the threshold p_{th} above/below which the RIO oscillation does/does not occur. The nominal PMR configuration is defined by alignment of the pendulum tip and the disk

center. Thus the nominal relative angles are given by $2\phi_{1o} = -\phi_{2o} = 82.82\text{deg}$. The other parameters a_i and b_i in the sensory signal conditioners φ_i are roughly determined so that a reasonable pendulum oscillation provides almost saturating inputs to the RIOs of magnitude comparable to the threshold of the neuron model ($a_1 = a_2 = 0.1$, $b_1 = 6$, $b_2 = 2$).

Once the structure of the CPG-based controller is fixed from biological observations, the essential design parameters of the controller are the feedback gain κ and the base frequency ϖ of the RIO. In the following, we will study the locomotion properties for various values of κ , ϖ , and the friction coefficient c .

A. Decentralized coordination

We fix the parameters c and ϖ to be $c = 50$ and $\varpi = 1$. If the gain κ is small, the connection between the PMR and the CPG is weak, and hence the RIOs oscillate near the base frequency ϖ as in Fig. 3, and the double pendulum oscillates with a small amplitude with no locomotion observed in the steady state. When the gain is increased above a threshold value, the tip of the double pendulum starts to encircle the disk center, resulting in locomotion of the PMR. That is, the average value of the disk velocity $\omega_o := \dot{\theta}_o$ is nonzero over a period. Such locomotion is observed when $1.6 \leq \kappa \leq 3.1$. If the gain is further increased, the double pendulum goes “wild” and a chaotic motion results (without locomotion).

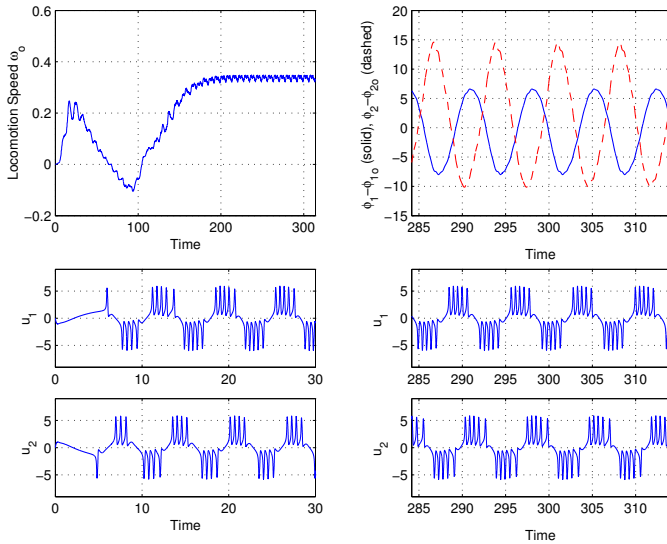


Fig. 5. Decentralized RIOs achieve locomotion (time responses)

Fig. 5 shows the time responses for the case $\kappa = 3$. We see that the double pendulum enters, after an initial transient, the steady state where the relative angles ϕ_1 and ϕ_2 oscillates in a sinusoid-like manner with a constant phase difference. As a result, the locomotion speed ω_o is periodic with a large bias and small fluctuations. The activities of the RIOs can be seen from the torque plots. Note in particular that the two

RIOs are just out of phase with each other at the beginning, but they become coordinated through the sensory feedback in the steady state. The corresponding steady state trajectory of the tip of the double pendulum is shown in Fig. 6 where the tip moves clockwise.

In summary, the CPG of decentralized structure is capable of coordinating the pendulum motion and inducing locomotion of the PMR with the aid of sensory feedback, as expected from the biological observation of leech swimming.

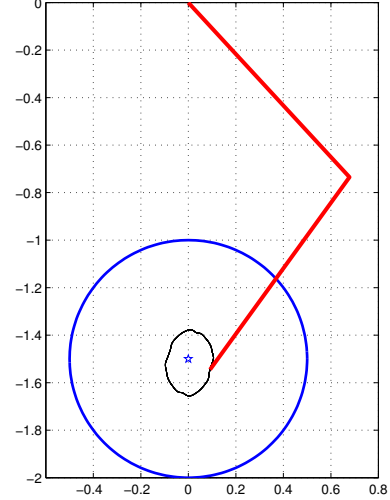


Fig. 6. PMR and its tip trajectory

B. Optimality

In this section, we shall examine efficiency of the PMR locomotion achieved by the CPG. As a measure of efficiency, we adopt the average value of the tip speed $\|v_{\text{tip}}\|$ of the pendulum, and the efficiency of the CPG-based controller will be compared with that of the statically optimal locomotion discussed in Section II-C.

The friction coefficient is fixed as $c = 100$ (for different values of c roughly in the range $50 \leq c \leq 200$, one can obtain similar results to those presented below), and the other parameter values are as given before. We have gridded the parameter plane (ϖ, κ) and identified the region where the controller achieves locomotion. Fig. 7(a) shows this region with contours of the achieved locomotion speed ω_o .

For each grid point on the (ϖ, κ) plane, the average value of the pendulum tip speed $\|v_{\text{tip}}\|$ and the locomotion speed ω_o are calculated whenever locomotion is achieved. These values define a point on the $(\omega_o, \|v_{\text{tip}}\|)$ plane which is marked by a dot in Fig. 7(b). The straight line in the figure shows the $\omega_o - \|v_{\text{tip}}\|$ relation for the statically optimal locomotion ($\|v_{\text{tip}}\| = 2\omega_o/\sqrt{c}$). The lower right boundary of the set of the dots (marked by ‘*’) gives the Pareto-optimal points on which no other choice of the controller parameters exists to achieve the same locomotion speed with less control

effort measured by $\|v_{\text{tip}}\|$. The Pareto-optimal curve is fairly close to the statically optimal line.

The parameter values corresponding to the Pareto-optimal points are marked by ‘*’ in Fig. 7(a). We see that the best feedback gain, for a given base RIO frequency ϖ , is given by the maximum value of κ for which locomotion occurs. This indicates the lack of robustness of the Pareto-optimal controllers with respect to the gain perturbation. Fig. 7(c) shows the relation between the pendulum frequency¹ ω and the locomotion speed ω_o . The Pareto-optimal cases indicated by ‘*’ are well aligned with the statically optimal relation $\omega = 2\omega_o$. Fig. 7(d) shows the orbit of the pendulum tip during locomotion for different values of κ where ϖ is fixed as $\varpi = 2$. As the gain κ gets larger, the orbit becomes larger, and just before losing locomotion, the orbit is of size comparable to the statically optimal orbit indicated by the dashed circle (the radius is $1/\sqrt{c} = 0.1$).

In summary, we have found that (i) the Pareto-optimal feedback gain κ is always at the upper boundary of the parameter region for guaranteed locomotion on the (κ, ϖ) plane, and in which case, (ii) the RIO-based controller can achieve the performance close to the static optimum as measured by the average speed of the pendulum tip.

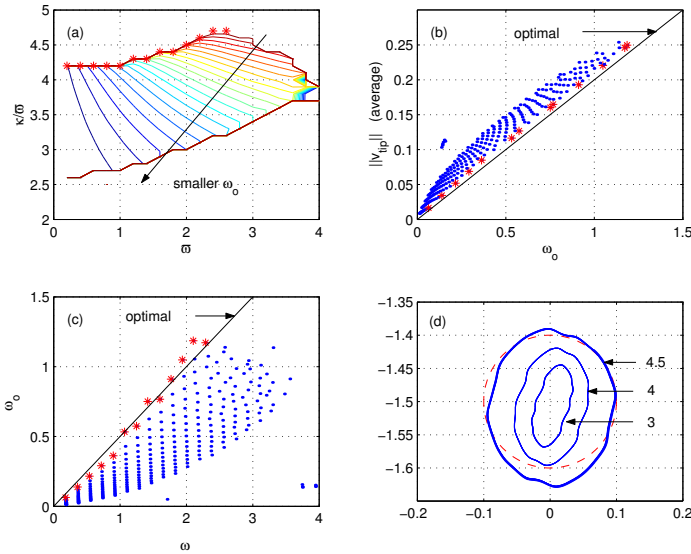


Fig. 7. Properties of CPG-induced PMR locomotion

V. CONCLUSION

We have examined the property of the CPG-based feedback controller with a decentralized structure in the context of driving a PMR that captures the essential dynamics of animal locomotion. The main findings in this paper can be summarized as follows:

¹The pendulum frequency ω is always found close to 0.9ϖ regardless of the feedback gain κ .

- The decentralized controller is capable of inducing locomotion of the PMR for a range of the feedback gain values κ and the RIO base frequency ϖ .
- The controller yields reasonable PMR locomotion in the sense that a given locomotion speed is achieved without excessive control effort (the pendulum tip speed), when compared with the statically optimal trajectory.

Numerous issues still remain for further investigation, including: (i) the effect of gravity, moment of inertia of the disk, and the ratio of the link lengths; (ii) the importance of neuronal dynamics in RIOs to generate spike trains with adaptation, (iii) the benefit of a direct communication path between the RIOs.

APPENDIX

RIO parameters

$$\begin{aligned} \gamma_v &= 2/0.544, \quad \gamma_t = 2\pi/(186.8\varpi), \\ \tau_v &= \gamma_t/\gamma_v, \quad \tau_w = \gamma_t/0.3, \quad q_o = -0.2, \quad v_o = -0.35\gamma_v, \\ a &= 1.8/\gamma_v, \quad b = 3/\gamma_v, \quad c = 2.2, \quad d = 5/\gamma_v, \\ k &= 10\gamma_t, \quad \tau_1 = 10\gamma_t, \quad \tau_2 = 100\gamma_t, \quad \sigma = 8/\gamma_v. \end{aligned}$$

- [1] B. D. O. Anderson. Personal communication. 1998.
- [2] C. Koch and I. Segev. *Methods in Neuronal Modeling: From Synapses to Networks*. The MIT Press, 1989.
- [3] G. N. Orlovsky, T. G. Deliagina, and S. Grillner. *Neuronal Control of Locomotion: From Mollusc to Man*. Oxford University Press, 1999.
- [4] W. O. Friesen and J. A. Friesen. *NeuroDynamix: Computer models for neurophysiology*. Oxford University Press, 1994.
- [5] F. Delcomyn. Neural basis of rhythmic behavior in animals. *Science*, 210:492–498, 1980.
- [6] X. Yu, B. Nguyen, and W. O. Friesen. Sensory feedback can coordinate the swimming activity of the leech. *J. Neurosci.*, 19(11):4634–4643, 1999.
- [7] T. G. Brown. The intrinsic factors in the act of progression in the mammal. *Proc. Roy. Soc. Lond.*, 84:308–319, 1911.
- [8] W. O. Friesen. Reciprocal inhibition: A mechanism underlying oscillatory animal movements. *Neurosci. and Biobehav. Rev.*, 18(4):547–553, 1994.
- [9] J. H. Koteleski, S. Grillner, and A. Lansner. Neural mechanisms potentially contributing to the intersegmental phase lag in lamprey. *Biol. Cybern.*, 81:317–330, 1999.
- [10] M. Saito, M. Fukaya, and T. Iwasaki. Serpentine locomotion with robotic snake. *IEEE Control Systems Magazine*, 22(1):64–81, 2002.
- [11] P. Prautsch, T. Mita, and T. Iwasaki. Analysis and control of a gait of snake robot. *Trans. IEEJ, Industry Appl. Soc.*, 120-D(3):372–381, 2000.
- [12] A. L. Hodgkin and A. F. Huxley. Currents carried by sodium and potassium ions through the membrane of the giant axon of loligo. *J. Physiol.*, 117:500–544, 1952.
- [13] T. Iwasaki and M. Zheng. The Lur’e model for neuronal dynamics. *Proc. IFAC World Congress*, 2002.
- [14] T. Iwasaki and M. Zheng. The Lur’e framework for modeling and analysis of neuronal oscillator. *IEEE Trans. Auto. Contr.*, 2003. (Submitted).
- [15] T. Iwasaki. Robust self-excitation by biological oscillators. *Proc. IFAC World Congress*, 2002.
- [16] T. Iwasaki and M. Zheng. What makes the biological oscillator achieve robust self-excitation? *Proc. American Contr. Conf.*, 2003.